Multiple Functions of Cancer Targeting, Imaging and Photothermal Therapy by Au-based Theranostics Released from Advanced Tissue Engineering Scaffolds

Lin Guo, Min Wang
Department of Mechanical Engineering, The University of Hong Kong, Pokfulam Road, Hong Kong
Email: memwang@hku.hk

Introduction: Current diagnostic and therapeutic methods for cancers are various. However, high cancer recurrence rates threaten human lives, early detection and effective treatment are therefore vital for post-surgery cancer patients. Gold nanoparticle (AuNP)-based theranostics are considered as one of the most attractive nanodevices for both detection and treatment for cancer due to their unique properties such as surface enhanced Raman scattering (SERS) effect [Xie J, *et al*., *Adv Drug Deliver Rev*, 2010, 62:1064-1079.]. The strongly amplified Raman signals can be used for high-sensitivity cancer detection and phothermal therapy can be simultaneously achieved on account of the ability to concert light into heat to provide overheating on cancer cells. In addition, new tissues need to be formed at the original tumor site after surgical removal and scaffolds-based tissue engineering possesses advantages for the tissue regeneration [Hollister S J. *et al*., *Nat Mater*, 2005, 4:518-524.]. In this study, advanced scaffolds incorporated with theranostics-encapsulated microspheres were fabricated, aiming to achieve both tissue regeneration and early detection and treatment for recurrent cancer at the same time. The characterization and biological performance including cancer cell targeting, imaging and phothermal therapy were evaluated.

Methods: Core-shell structured folic acid-chitosan-capped gold (Au@CS-FA) NPs were synthesized using a one-pot synthesis method [Guo L, *et al*., *Proc. 10th WBC*, Montreal, Canada, 2016]. FA would provide specific targeting ability of cancer cells. For cancer detection, rhodamine 6G (R6G) was embedded in NPs for generating SERS signals. In order to obtain controlled release of theranostics, co-axial electrospray was used to fabricate core-shell structured PLGA 50/50 microspheres to encapsulate theranostics and release gradually as microspheres degraded. Advanced scaffolds incorporated with theranostics-encapsulated microspheres were produced by concurrent electrospinning and co-axial electrospray. Various techniques (TEM, SEM, UV-Vis, etc.) were used to characterize synthesized NPs, microspheres and advanced scaffolds. The SERS activity of NPs both before encapsulation and after release was measured using Raman spectroscopy. *In vitro* immersion tests of the advanced scaffolds were conducted. For biological investigations, including cancer cell targeting, *in vitro* SERS detection and photothermal therapy, HeLa cells with high folate receptor (FR) expression were used and MCF-7 cells were chosen as negative control.

Results: Synthesized NPs possessed core-shell structure with many irregular tips on the Au core and a thin layer of CS-FA. Theranostics-encapsulated microspheres with uniform size were successfully fabricated and EDX spectrum indicated the existence of Au, which confirmed that the AuNP-based theranositcs were encapsulated in microspheres. SEM results showed that the core-shell structured microspheres randomly distributed in advanced scaffolds (Fig.1a). After immersion in PBS, the advanced scaffolds degraded and controlled release of theranostics occurred when microspheres broke through biodegradation. TEM image indicated the intercellular uptake of released theranostics in HeLa cells and the theranostics remained original morphology and structure (Fig.1b). SERS spectra was displayed in Fig.1c. The intensity of Raman signals were still significantly enhanced when theranostics were released from scaffolds. Dark-field and fluorescent images of HeLa cells after incubation with the advanced scaffolds were shown in Fig.2a and Fig.2b. HeLa cells were covered with strong yellow light scattered from released theranostics, comparing with very weak light from MCF-7 cells. Under fluorescent microscope observation, the nucleus of cells showed blue fluorescence (stained by DAPI) and bounded theranostics around the HeLa cells showed strong red fluorescence due to the embedded R6G, however, only very weak signals could be found in MCF-7 cells. For photothermal therapy, Live/Dead viability assay was conducted after NIR irradiation and stained cells were observed under fluorescent microscope. A well-defined circular zone of dead cells was displayed in HeLa cells after incubation with advanced scaffolds and irradiation by laser (Fig.2c). HeLa cells irradiated under the same conditions but incubated with theranostics-free scaffolds maintained cell viability with lack of red fluorescence. These results indicated that the theranostics-incorporated scaffolds possess capability for cancer targeting, imaging and phothermal therapy for cancer patients.

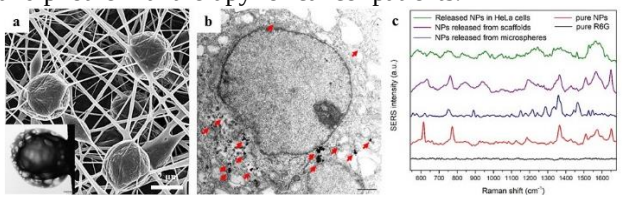

Fig. 1. Properties of advanced scaffolds and released theranostics: (a) SEM image (insert in a: TEM image of core-shell structured microspheres), (b) TEM image of released theranositcs in HeLa cells, (c) SERS spectra.

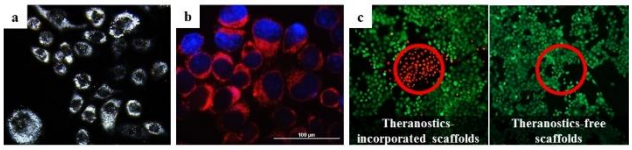

Fig. 2. Biological assessments of released theranostics in HeLa cells: (a) dark-field image, (b) fluorescent image, (c) live/dead assay results after NIR irradiation with theranostics-incorporated and theranostics-free scaffolds.

Conclusions: The advanced scaffolds with incorporation of Au-based theranostics-encapsulated microspheres were successfully fabricated. *In vitro* biological results demonstrated that released theranostics from the advanced scaffolds exhibited good cancer targeting and optical ability and combined photothermal therapy.